A FENESTRON MODEL FOR IMPROVING THE HELICOPTER YAW DYNAMICS FLIGHT SIMULATION

P.-M. Basset

Senior Research Engineer

M. Brocard

Graduate Student

System Control and Flight Dynamics Department, ONERA

Salon-de-Provence, FRANCE

Nomenclature

b	number of blades,
c	blade chord, (m)
$C_{L\alpha}$	blade airfoil lift curve slope, (deg^{-1})
DTA	tail rotor collective pitch angle, (deg)
DR	yaw acceleration, (deg/s^2)
r	radial position of a blade element, (m)
R	rotor radius, (m)
R_{Hel}	yaw rate, (deg/s)
S	fan disk surface, (m^2)
T_{FAN}	Fan thrust, (N)
T_{Fen}	Fenestron total thrust, (N)
T_{Shroud}	Shroud thrust, (N)
V_0	upstream airspeed, (m/s))
V_1	axial airflow through the fan, (m/s)
V_2	downstream airspeed, (m/s)
V_i	rotor induced velocity, (m/s)
V_R	upcoming airspeed normal to the fan, (m/s)
V_T	translation speed, (m/s)
V_{TD}	Deviated translation speed, (m/s)
θ	collective pitch, (deg)
ρ	air density, (kg/m^3)
σ	fenestron wake contraction factor
τ_S	time constant of the shroud thrust, (s)
Ω	rotor rotational speed, (rad/s)

Presented at the 30th European Rotorcraft Forum, Marseilles, France, September 14-16, 2004.

Abstract

Most of the helicopter flight dynamics simulation models overestimate the yaw response to pedal inputs. This issue is presently addressed by a GARTEUR group HC-AG11 on "Yaw axis dynamics". Within this group, ONERA investigates now more precisely the modelling of the fenestron or "fan-in-fin". The modelling of this ducted fan is more complex than a classical tail rotor because of the shroud-fairing. The paper presents some significant improvements of the fenestron modelling allowing a better simulation of the yaw dynamics. The simulation are compared with respect to flight test data on a Dauphin helicopter.

Introduction

The fenestron (small round window in French) is a ducted fan also called fan-in-fin replacing the classical tail rotor. First installed on the Gazelle helicopter in 1968, the concept was initiated and developed (e.g. Ref. 1-3) by EuroCopter (formerly "Division Hélicoptère" within "Sud Aviation" then in "Aérospatiale"). The EC helicopters equipped with a fenestron are the Dauphin, EC120 Colibri, EC130, EC135 for the civil ones, and Fennec (EC130B4), EC635, Panther (AS565) for the military versions. Since the fenestron brevet was in the public domain, the concept has been applied by other constructors like Mitsubishi 2000 and Kawasaki for the Japanese helicopters, Kamov KA 60 and 62 for the Russian, Boeing-Sikorski RAH-66 Comanche for the USA.

The goal of this paper is not to discuss the pros and the cons of the fenestron which were summarised in (Ref. 4-5). The main advantage with respect to a classical tail rotor is that the fan blades are surrounded by a duct or shroud fairing which improves the safety of the persons on the ground and of the helicopter itself.

State of the art

The study presented here aims at enhancing the model used in the rotorcraft simulation codes for computing the dynamic thrust developed by the fenestron. This model is dedicated to the applications requiring the simulation of the flight dynamics. The models based on CFD methods for describing the streamlines and pressure distribution around the fenestron are more devoted to aerodynamics and aeroacoustics like the ONERA work presented in (Ref. 6) for the computation of the noise of the Dauphin fenestron.

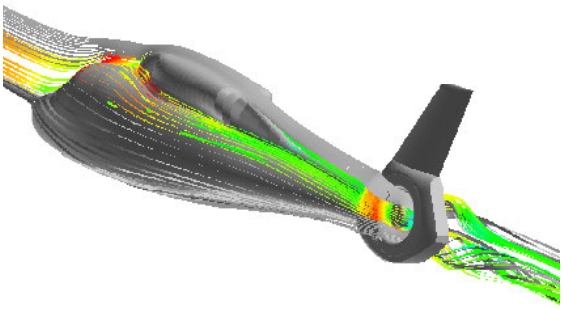

Figure 1 : ONERA CFD computation of the streamlines along the fuselage of a Dauphin and through its fenestron in forward flight at 150 kt.

However some studies like the ones performed for the FanTail of the RAH-66 Comanche deals with the yaw flight mechanics (Ref. 7-8). But these studies are still often focused on trimmed flight condition : the stationary flow field through the FanTail is computed for a given fan collective pitch in steady flight condition (hover, sideward, forward flights), moreover the contribution of the main rotor is not taken into account. In (Ref. 7) the fan is idealised as momentum sources which are time averaged on one revolution for the given number of blades. In (Ref. 8) the fan is modelled as an actuator disk with two options. With uniform momentum theory, the uniform pressure jump is computed directly from the fan thrust set as an input. With blade element theory, the time average pressure jump at a given point on the rotor disk is computed from the local blade element lift. The dynamics of the thrust response due to variation of the blade pitch or of the external flow (flight maneuver, main rotor wake, gust, etc.) are not considered in these CFD approaches. On the other hand, a more analytical method is presented by the Kamov company in (Ref. 9) for computing the performance (thrust, figure of merit) of the ducted tail fan of the Ka-60 helicopter in hover. The paper provides analytical expressions to assess the influence of the shroud on the fan-in-fin wake and thrust. But again no dynamics is considered and only the hovering condition is dealt with.

Our purpose being to improve the simulation of the flight dynamics of helicopters equipped with a fenestron, the thrust model must be simple enough to be implemented in a comprehensive rotorcraft flight dynamics code and it must take into account the thrust dynamics. Very few papers deal with this topic. In (Ref. 10), a parametric optimisation algorithm integrated by ONERA in the simulation code H.O.S.T. ("Helicopter Overall Simulation Tool") was applied by DLR for improving the yaw dynamic simulation of the EC135. An extra term proportional to the yaw rate was added to the fenestron thrust :

$$T_{Fen} = T_{Fen} + K_T . R_{Hel}$$

The idea was to increase the yaw damping with a direct feed-back of the yaw rate on the fenestron thrust. Even by imposing the same roll rate as in the flight test, the optimisation of K_T to minimise the discrepancy between simulation and flight test, did not allow to match well the yaw rate response. The author concluded that a new comprehensive formulation of the fenestron model should be considered in an integrated analytical / parametric approach.

The published analysis which is the closest to our study, is the one reported in (Ref. 11) for the Comanche's Fantail although more related to handling qualities (frequency domain investigation). The main assumptions are the following :

- no wake contraction,
- the forward speed V_T does not enter in the expression of the fan thrust,
- after passing through the ducted fan, the wake is turned back into the direction of the freestream (no "flying pipe shape" as could be assumed for a high loaded ducted fan in the role of a main rotor, Ref. 12).

This approach of the problem may be sketched as follows with (*v*) being the mean inflow (V_{im}) :

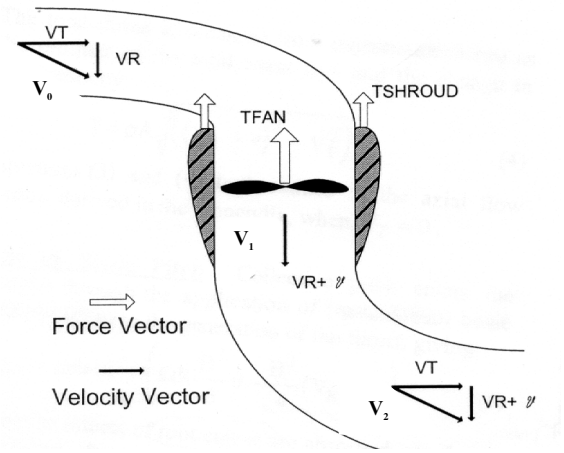

Figure 2 : Concept sketch of the ducted fan model from (Ref. 11).

The total thrust (Tfan + Tshroud) developed by the ducted fan is calculated by momentum theory :

$$T = \rho.S.\sqrt{{V_T}^2 + (V_{im} + V_R)^2}.V_{im} \qquad (1)$$

The translation speed (V_T) is taken into account in this global term. The only unknown is the mean inflow (V_{im}) which is calculated by equating two expressions of the fan thrust :

- one coming from Bernoulli's equation upstream and downstream the fan :

$$T_{FAN} = \rho.S.\left|V_R + \frac{V_{im}}{2}\right|.V_{im} \qquad (2)$$

- the other is a global expression coming from the (quasi-steady) blade element theory in order to make appear the collective pitch, as can be found in (e.g. Ref. 13) :

$$T_{FAN} = \rho.b.c.\Omega.R^2.\left(\Omega.R.\frac{B^3}{6}.\theta - (V_R + V_{im}).\frac{B^2}{4}\right).C_{L\alpha} \qquad (3)$$

as usual (B) is the tip loss factor and the (θ) is the value of blade pitch at the three-quarter radius.

An unsteady version of the model is proposed by adding two dynamic mean inflow terms: $\left(\rho.S.H_M.\dot{V}_{im}\right)$ in the total thrust expression (1) and $\left(\rho.S.H_F.\dot{V}_{im}\right)$ in the fan thrust expression (2). (H_M) can be seen as the height of the cylinder of air which must be accelerated by the ducted fan to produce the total thrust (T). (H_F) can be seen as the height of the cylinder of air which must be accelerated by the fan only to produce the fan thrust (T_{FAN}). For a classical (open) rotor, the dynamic inflow theory (e.g. Ref. 14) gives $\left(H_R \cong \frac{8.R}{3.\pi}\right)$. For a ducted fan, it is proposed to identify these values from experimental data. The value of (H_F) providing the best match with the measured frequency response seems to be (2.5.R) according to (Ref. 11) which does not precise for which value of (H_M). This tuned value is higher than the theoretical value of (H_R).

The initial model from which this study starts, is the one used in the H.O.S.T. simulation code ("Helicopter Overall Simulation Tool" created by EuroCopter and developed with contributions of ONERA). Several levels of modelling are available in HOST for the fenestron. But if we exclude the simplest one and the one interpolated on wind-tunnel test, the remaining model is based on a similar approach as presented in (Ref. 11). Indeed, the inflow through the fan is searched as the crossing of two theories : the modified momentum theory and the blade element theory. Then knowing the airflow through the fenestron, the total thrust can be calculated.

However, if the principles are comparable with the concept of (Ref. 11), the initial model is different in each of these calculation steps.

First, the fan disk is radially discretised along the blade span in rings of width (Δr). The inflow is calculated on each of these rings and the thrust is the sum of their contribution (ΔT). Therefore the model is more suited to account for the variation along the blade span (twist, airfoils, etc.). Thus instead of a global expression as (3), a more local blade element theory is used.

Second, the wake contraction is considered in the computation of the airflow through each ring (modified momentum theory) and in the thrust expression. In the classical momentum theory for an open rotor, the contraction parameter is (σ = 0.5), whereas for a ducted fan the wake contraction is closer to one as shown below (Fig. 3) :

$$\sigma = \frac{\left\|\vec{V}_1\right\|}{\left\|\vec{V}_2\right\|}$$

with (V_1) being the airflow through the fan and (V_2) the airflow downstream where the wake is fully developed as sketched hereafter :

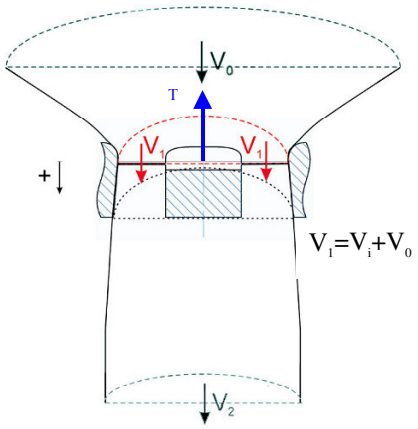

Figure 3 : Modified momentum theory for the ducted fan.

Third, in (Ref. 11) the translation speed (V_T) is taken into account in the total thrust expression (1), but not in the computation of the inflow through the fan (expressions (2) and (3)). In the initial model, for the blade element expression of the fan thrust, only the axial airflow is considered as in (Ref. 11) which seems to be realistic since the blade airfoils are not exposed to the translation speed. But the thrust expression coming from the modified momentum theory, takes into account the total incoming airflow (V_0). Indeed in the initial model, as regards the part coming from the momentum theory (both in the inflow equation and in the total thrust), the ducted fan is supposed to accelerate the flow in the axial direction as sketched on Fig. 4.

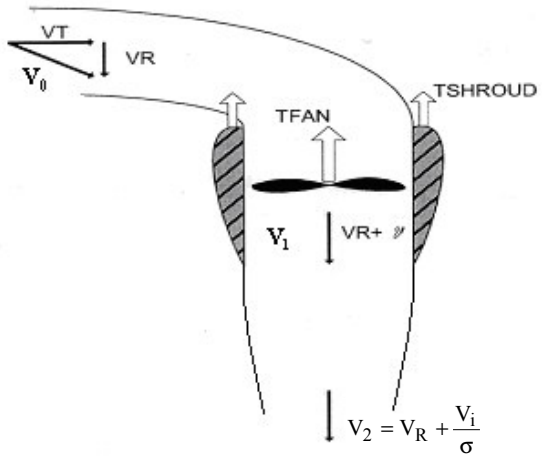

Figure 4 : Airflow through the ducted fan in the case where the induced flow is higher than the forward speed.

Fourth, in the initial model this scheme of the airflow (Fig. 4) is recognised to be valid when the induced flow is higher than the forward speed. When the translation speed is higher than the induced flow, the fenestron behaves more like a wing with a suction on the collector side and a transpiration on the exit side (Fig. 5).

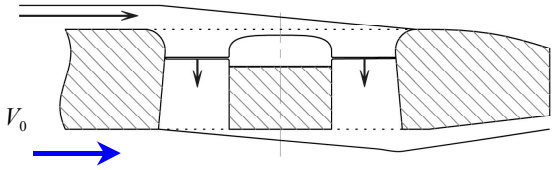

Figure 5 : Deviation of the airflow by the fenestron in high forward flight.

That is why in the initial model, the total thrust is the combination of both contributions :

- the part coming from the modified momentum theory (modified by a different wake contraction and an airflow pattern as

shown on Fig. 4) which is predominant at low speeds :

$$T_{z\_DuctedFan} = q.\left(V_{0z} - \frac{V_i}{\sigma_{max}} \right) \qquad (4)$$

- the part coming from the Prandtl theory for an elliptic wing which is predominant at high forward speeds :

$$T_{z\_Wing} = signe(V_i).2.q.\left\|\vec{V}_0\right\|.k(\varepsilon) \qquad (5)$$

with (q) the mass flow rate : $q = \rho.S.V_i$, and (k(ε)) is a transition term between the two contributions in order that (T_{z_Wing}) be null when $\left(\varepsilon = \frac{V_i}{V_0} \geq 1.5\right)$ i.e. :

$$\begin{cases} k(\varepsilon) = 1 - \frac{\varepsilon}{3/2}, \text{ pour } \quad \varepsilon = \frac{V_i}{V_0} < 3/2 \\ k(\varepsilon) = 0 \quad \text{, pour } \quad \varepsilon = \frac{V_i}{V_0} \geq 3/2 \end{cases} \qquad (6)$$

Furthermore in the initial model, the total thrust is a vector with terms (T_x) and (T_y). It also accounts for the sideslip angle. The purpose of the paper is not to describe the initial model in details, therefore only the main lines of this reference model have been drawn.

This model has been developed by EuroCopter in four steps :

- modelling of a ducted fan in hover,
- adaptation to straight forward flight,
- adaptation to forward flight with small sideslip,
- adaptation to forward flight with strong sideslip (lateral flights).

At each step of its conception, some empirical parameters have been identified with respect to steady wind-tunnel tests on a scale fenestron model. For example in hover, the model was found to yield a good match with the test data for a contraction parameter :

- if (V_1) is in the direction collector → diffuser : σ = 0.6,
- if (V_1) is in the direction diffuser → collector : σ = 0.3.

A law of variation of this contraction factor is used in the model to account for the effect of the ratio (ε = mean inflow / forward speed), sideslip angle, …

This initial model is good for trims, but overestimates the yaw dynamics as can be seen for example on Fig. 6-7.

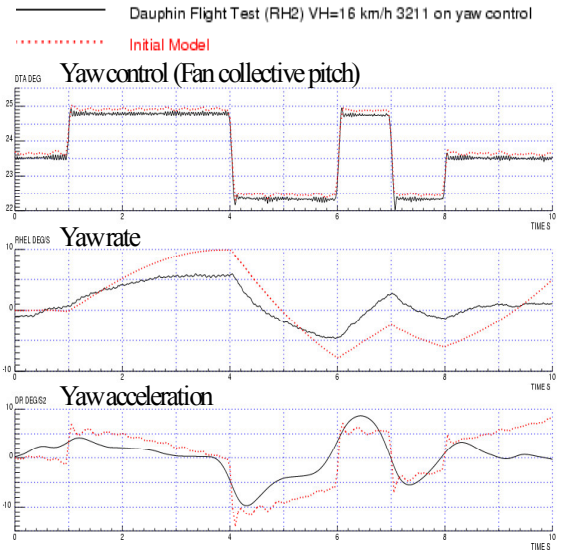

Figure 6 : Initial yaw dynamics near hover.

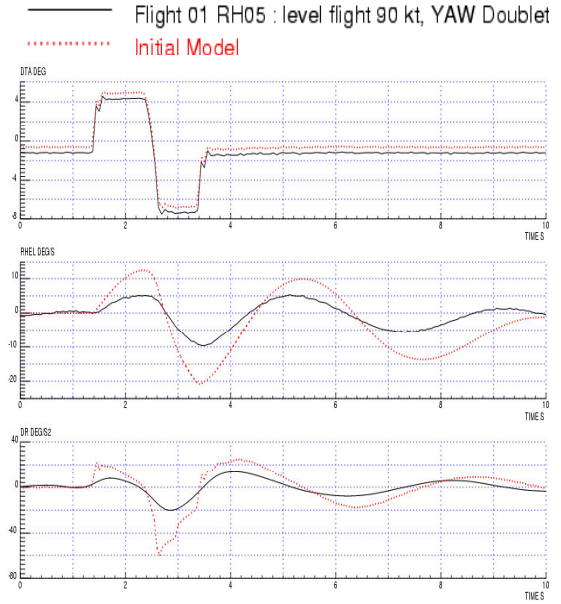

Figure 7 : Initial yaw dynamics at 90kt.

Knowing that the model has been developed on the basis of steady wind-tunnel tests, our contribution was first focused on the thrust dynamics as summarised hereafter.

The Dauphin SA365N and its fenestron

The flight test used in this study have been performed by the French flight test centre in Istres with the supervision of ONERA (e.g. Ref. 15). The considered helicopter is the Dauphin SA365N shown on Fig. 8.

Figure 8 : The Dauphin SA365N used for the French research flight test in Istres.

The fenestron of the Dauphin SA365N has 13 blades equally distributed around the hub and they turn such as the bottom blade goes forward. The shroud can be divided in two parts : the inlet (or collector) characterised by a lip with the curvature radius (r_{lip}) and the exit (or diffuser) which has an opening angle (α_{dif}).

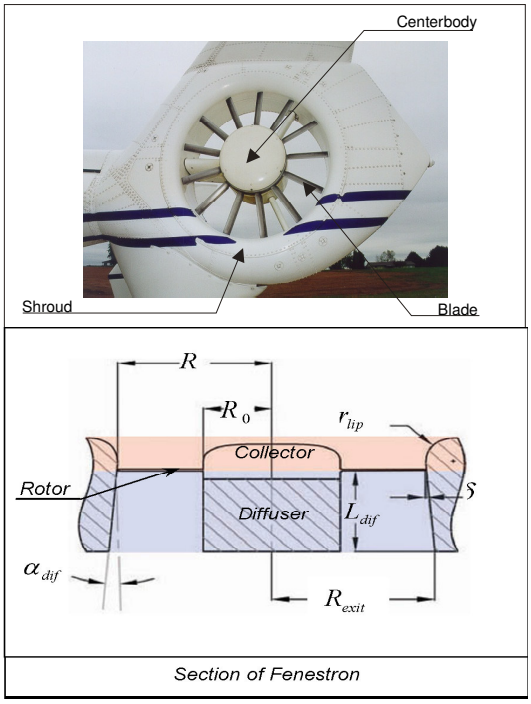

Figure 9 : The fenestron of the helicopter Dauphin SA365N.

For example in the case of a steady hovering, the fenestron developes a thrust oriented on the left side of the helicopter to counter the main rotor torque effect. By pushing on the right pedal, the collective blade pitch of the fenestron is increased and thus the thrust on the left, resulting in a nose right motion.

The database includes flights at different speeds from low speeds near hover until 140 kt with different kind of inputs on the yaw control (doublet, 3211, etc.).

Proposed Dynamic Fenestron Model

In order to improve the initial model for a better simulation of the yaw dynamic response to pedal inputs, the thrust formulation has been changed as well as the computation of the inflow through each of the rings discretising the fan.

Dynamic Shroud / Fan Thrust Formulation

First, the approach is to make a clear distinction between the contributions of the fan and of the shroud. In the initial model, the thrust term (T_{z_Wing}) can be seen as a shroud contribution in forward flight. But when the forward speed decreases, this term becomes null, whereas the shroud also contributes to the thrust at low speed. Indeed, near hover, the pressures on the lips of the shroud produce nearly the same thrust as the one resulting from the lift developed by the blades of the fan, as shown for example on Fig. 10 extract from (Ref. 3).

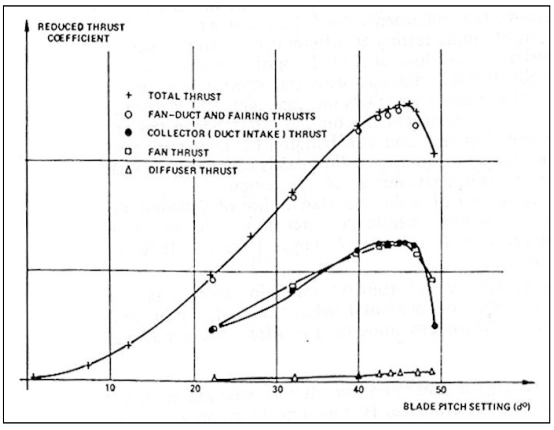

Figure 10 : Thrust sharing between Fan and Shroud –fairing (from Ref. 3).

So we propose to complete the direct contribution of the shroud to the thrust in hover and low speeds :

$$T_{FenestronQS} = T_{FanQS} + (1-k(\varepsilon)).T_{ShroudHoverQS} + k(\varepsilon).T_{ShroudForwardFlightQS} \quad (7)$$

k(ε) is the transition factor already used in the initial model (in hover k(ε)=0 and tends to 1 when the forward speed increases). The term ($k(\varepsilon).T_{ShroudForwardFlightQS}$) corresponds to ($T_{z\_Wing}$) (equation 5). The shroud thrust in hover ($T_{ShroudHoverQS}$), can be calculated with an analytical expression depending on the geometrical characteristics of the fairing (see Fig. 9). This formulation from (Ref. 9) being limited to the hover case, that is why the term (T_{z_Wing}) is kept for accounting for the effect of the shroud in forward flight.

$$T_{ShroudHoverQS} = \left(\frac{1}{1+\varepsilon_B.\left(\frac{K_V}{2} + \frac{(\xi_{col}+\xi_{dif})}{2.K_V} - 1 \right)} - 1 \right).T_{FanQS} \quad (8)$$

- (ε_B) is the blade tip clearance factor (see Fig. 9) : $\varepsilon_B = 1 - 109.\left(\frac{\delta}{R}\right)^{3/2}$
- (ξ_{col}) and (ξ_{dif}) are respectively the inlet and exit drag factors for which laws have been determined from experimental data depending on the shroud geometrical characteristics and on the sense of the thrust (positive or reverse directions).
- (K_V) is the velocity ratio (V_2/V_1) which is in fact the inverse of the contraction factor.
  - When $V_1>0$ (collector → diffuser) : $\sigma_c = \frac{1}{K_v} = n.(1+0{,}4.\alpha_{dif})$ with (α_{dif}) in radian and : $n = \frac{(2.R_{sdiv})^2}{(2.(R+\delta))^2}$ (in the case of the Dauphin SA365N, this value of the contraction factor in hover is : $\sigma_c \approx 1.16$).
  - When $V_1<0$ (diffuser → collector) : $\sigma_c = 1$

As mentioned, in the initial model this contraction factor was tuned to better match the test data in hover. By this way the fan thrust was adjusted (even if all the thrust was not due to the fan). But since now we add a shroud thrust in hover, it is preferable to use the analytical expression of the contraction (σ_c) derived from (Ref. 9) for a less empirical fan thrust. Besides the contraction factor is thus interestingly expressed in function of the geometrical characteristics of the fenestron.

Then, ONERA has introduced two first order equations for the computation of the thrust of the fan and the thrust of the shroud respectively. The use of two different time constants was first proposed in order to account for the fact that : the thrust developed by the blades reacts more rapidly to blade pitch inputs than the thrust resulting from the change of pressure distributions around the shroud. But it turns out that the fan thrust reacts so rapidly that it can be considered as quasi-static. A first order dynamic equation can be kept for the shroud thrust for reflecting the fact that the pressure distribution around the lips of the fairing reacts with a time lag (τ_s) after any aerodynamic change through the fan (e.g. a blade pitch variation).

$$\tau_S.\dot{T}_S(t) + T_S(t) = T_{ShroudQS}(t) \quad (9)$$

with :

$$T_{ShroudQS} = (1-k(\varepsilon)).T_{ShroudHoverQS} + k(\varepsilon).T_{ShroudForwardFlightQS} \quad (10)$$

The point of application of the shroud thrust is also subject to improvement because that could change the yaw moment transmitted to the helicopter centre of gravity. Some wind tunnel measurements which confirmed the physics, have shown that the shroud thrust is above all developed on the fore part of the fairing. This reduction of the lever arm with respect to the helicopter centre of gravity would tend to decrease the variation of the fenestron yaw moment in response to a pedal input.

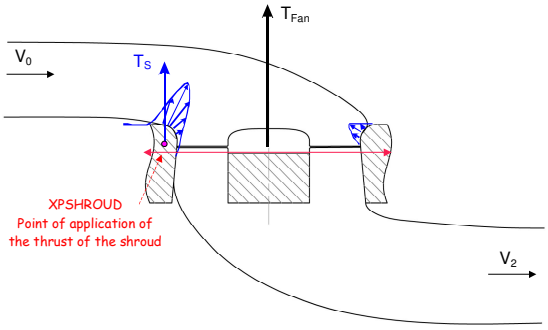

Figure 11 : Point of application of the resulting shroud thrust.

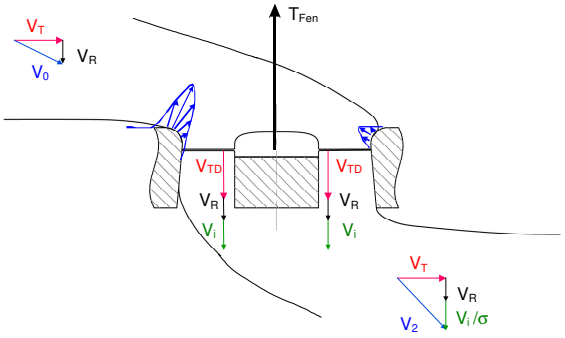

Figure 12 : Deviation of the airflow through the fenestron.

But even with the assumption that the point of application of the shroud thrust is at the most forward position on the front part of the fairing, the effect is negligible on the yaw dynamics. Therefore the assumption that the shroud thrust is applied at the centre of the fenestron can be kept for flight mechanics applications.

Inflow computation

The force applied by the fan thrust on the airflow corresponds to the total change in the momentum from the upstream where the speed is $(\vec{V}_0)$ to the downstream where the airspeed is $(\vec{V}_2)$:

$$\vec{F} = Q.(\vec{V}_2 - \vec{V}_0)$$
$$= Q(\vec{V}_R + \frac{\vec{v}_i}{\sigma} + \vec{V}_T) - Q(\vec{V}_R + \vec{V}_T) = Q.\frac{\vec{v}_i}{\sigma} \quad (11)$$

Here is proposed a new expression for (Q), the mass flow rate through the fan :

$$\boxed{Q = \rho.S.(V_{TD} + v_i + V_R)} \quad (12)$$

where (V_{TD}) is the deviated translation speed into the fenestron. Indeed, it can be considered that depending on the ratio between the inflow through the fan and the translation speed, a part of the upcoming airflow $(\vec{V}_0)$ is redirected axially through the fenestron and then deviated into $(\vec{V}_2)$ as sketched on (Fig. 12).

As for the thrust calculation, the k(ε) transition factor can be used to reflect that when the inflow through the fan is higher than the forward speed, the upcoming air particles are deviated into the fan with their convection speed (V_T) transformed axially into (V_{TD}). But when the forward speed is higher than the inflow, only a few part of the upstream airflow is axially deviated into the fan. Therefore we propose to use :

$$\boxed{V_{TD} = (1 - k(\varepsilon)).\sqrt{V_0^2 - V_R^2} = (1 - k(\varepsilon)).V_T} \quad (13)$$

This deviated airflow is also used in the fan thrust calculated by the blade element theory. It enters into the blade element angle of attack calculation and in the local airspeed at the radius (r). Therefore the following equation is used for the computation of the inflow through each of the rings composing the fan disk (at the radial station r) :

$$\boxed{\frac{1}{2}.C_{L\alpha}(\theta - \alpha).b.c.\cos\alpha.((V_i + V_R + V_{TD})^2 + \omega^2 r^2) - 2.\pi r.(V_i + V_R + V_{TD}).\frac{V_i}{\sigma} = 0} \quad (14)$$

Thus this concept of the airflow behaviour through the fan, insures the coherence between the blade element and the modified momentum theory expressions and also a satisfying consistency between the inflow computation and the thrust formulation.

Two dynamic inflow equations were also tried. One is based on the Pitt and Peters model (Ref. 14, reduced here to the mean inflow) in which the translation speed is taken into account as for an open rotor. That leads to a time delay :

$$\tau = \frac{8.R}{3.\pi}.\frac{1}{2\sqrt{{V_T}^2 + (v + V_R)^2}}$$

whereas in the ducted fan model presented in (Ref. 11, "Comanche FanTail model"), the time lag on the mean inflow is :

$$\tau = \frac{8.R}{3\pi}.\frac{1}{\left|V_R + \frac{v}{2}\right|}$$

The HOST trim computations with each of these models for a swept on the forward speed in straight and steady level flights (V_T = forward speed and V_R=0) provide an order of magnitude of these time constants (Fig. 13).

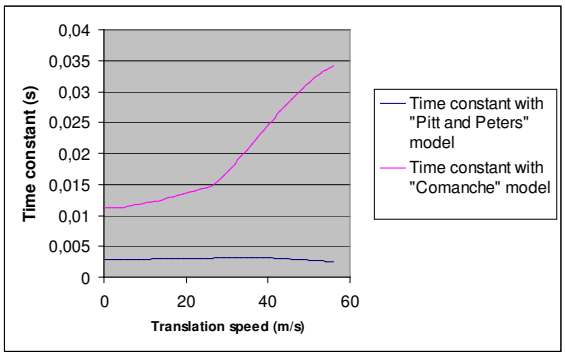

Figure 13 : Evolution of time constant with forward translation speed.

These values of the time lag on the inflow are very low. Taking them into account leads to small differences on the transitory response of the fenestron thrust. Therefore it can be concluded that the inflow variation in response of a blade pitch variation can be considered as quasi-static for the flight dynamics simulation.

Results and comparisons with flight tests

In the new model described previously, two parameters were found to have a significant impact on the yaw dynamics :

- the contraction factor (σ) in the inflow equation (14),
- the time lag (τ_s) in the shroud thrust establishment (equation 9).

For the following figures (14-19), the yaw inputs are the same as those presented on Fig. 6-7. The effect of the time constant (τ_s) at low forward speed (16 km/h) is shown on Fig. 14 and in forward flight at 90 kt on Fig. 15.

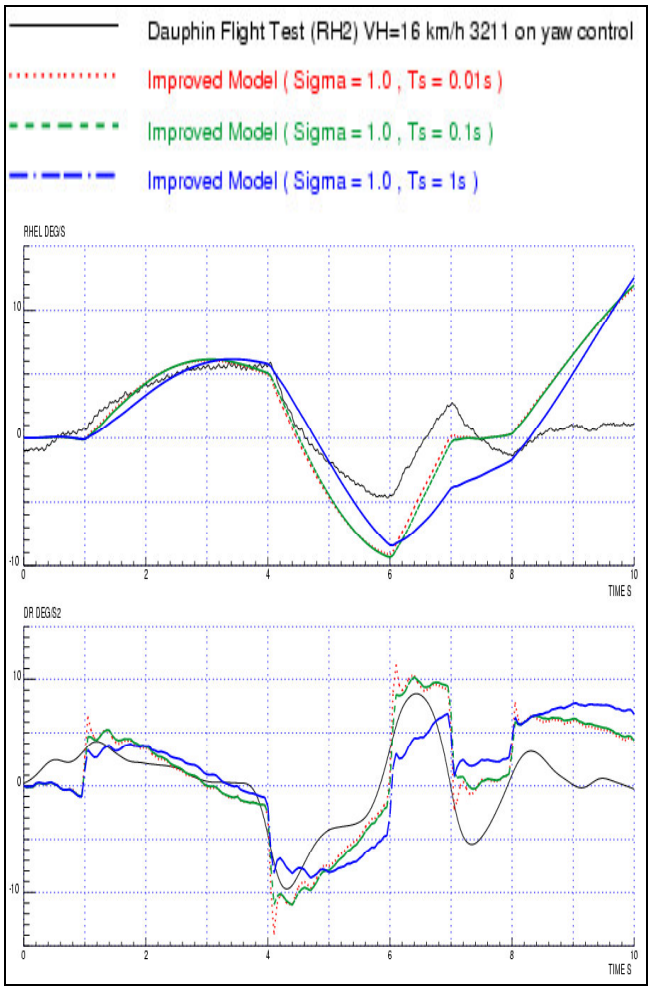

Figure 14 : Effect of the time constant (τ_s) near hover.

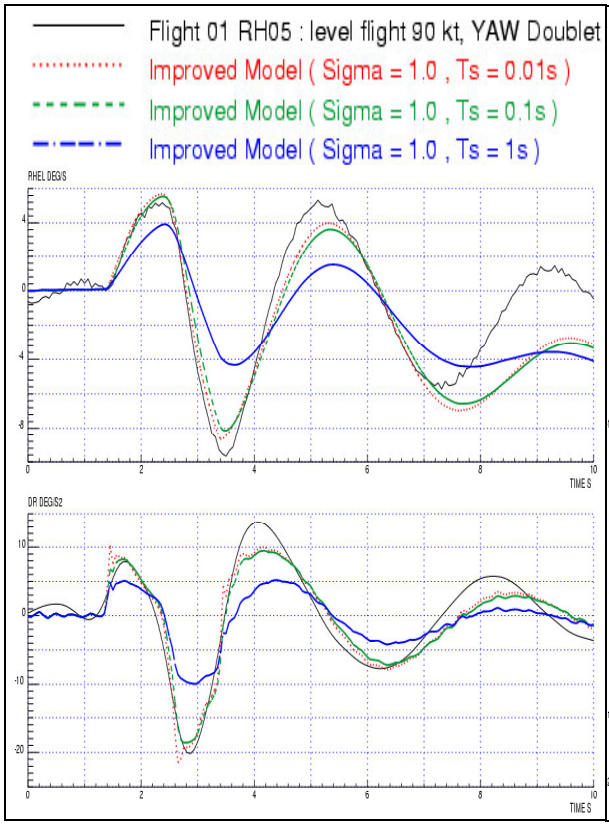

Figure 15 : Effect of the time constant (τ_s) in forward flight at 90kt.

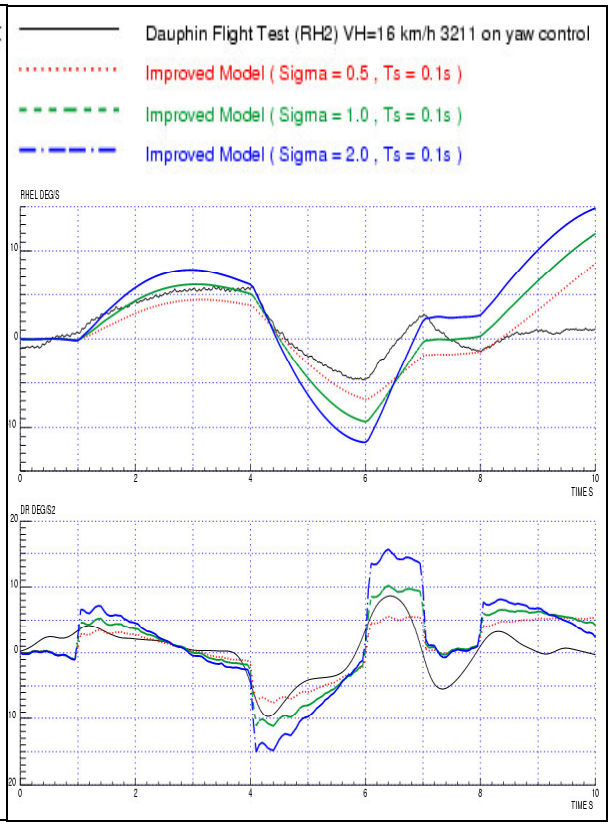

Figure 16 : Effect of the contraction factor (σ) at low forward speed.

Of course, the more the time lag is short, the more the yaw response reacts rapidly to the yaw control variation. For the following a time delay of (τ_s = 0.1s) was kept. The asymptotic behavior corresponding to the quasi-static case (τ_s = 0s) could also be retained if we consider the yaw rate. But regarding the yaw acceleration (DR), the transitory peaks seem too high in the case with a very low time constant (τ_s = 0.01s), although the flight test were filtered. Moreover the shroud thrust results from the pressure differences between the inlet and exit sides of the fairing. The physical common sense leads to consider that these pressure distributions take a certain time to establish after a blade pitch variation.

The effect of the contraction parameter (σ) at low forward speed (16 km/h) is shown on Fig. 16 and in forward flight at 90 kt on Fig. 17.

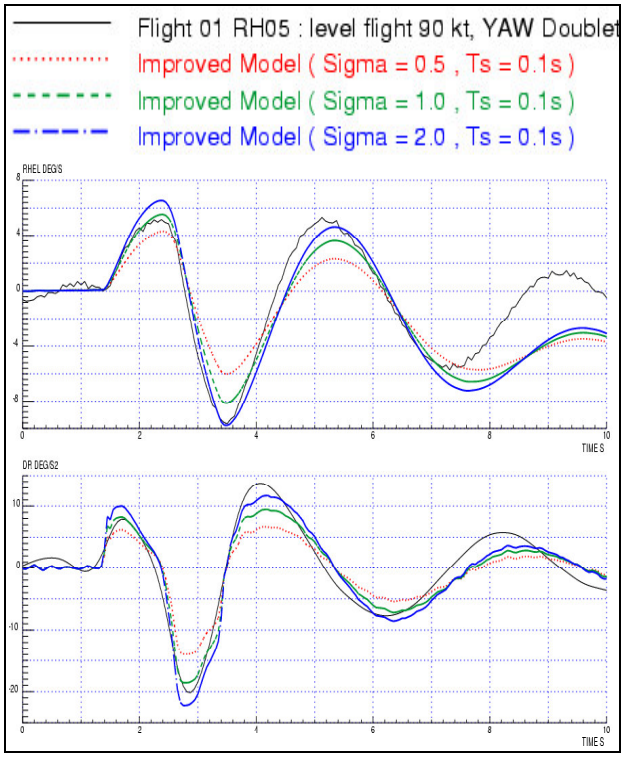

Figure 17 : Effect of the contraction factor (σ) in forward flight at 90kt.

The physical value of (σ) in the case of ducted fan in hover is close to one. As mentioned, the analytical expression of (Ref. 9) gives a value of (σ = 1.16) for our hovering fan-in-fin. But no results are available in forward flights. The new proposed model gives a good match with the flight test data with (σ = 1) near hover, but also in forward flight. Better correlation could be obtained by parametric optimisation, but here the purpose was to show the main tendencies. When (σ) increases, the yaw rate response is magnified, whereas decreasing (σ) leads to more yaw damping.

As shown on Fig. 18 and 19, the new fenestron model with (τ_s = 0.1s) and (σ = 1) improves significantly the yaw dynamics compared with the simulation results of the initial model.

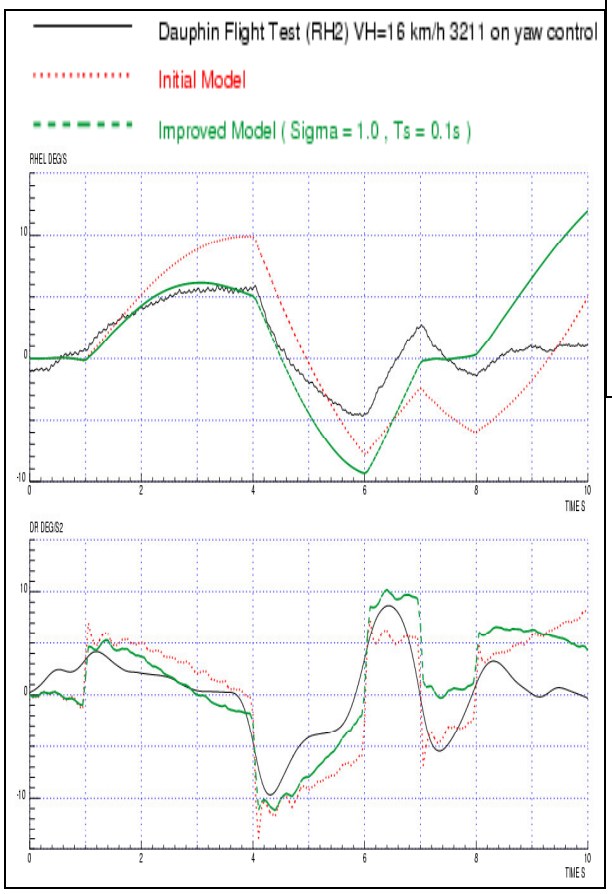

Figure 18 : Comparisons between HOST initial model and improved model near hover.

At low speeds (Fig. 18), the yaw input begins when the yaw acceleration is not null in the flight test (see also Fig. 6). The comparison with the simulation is therefore more tricky than in forward flight.

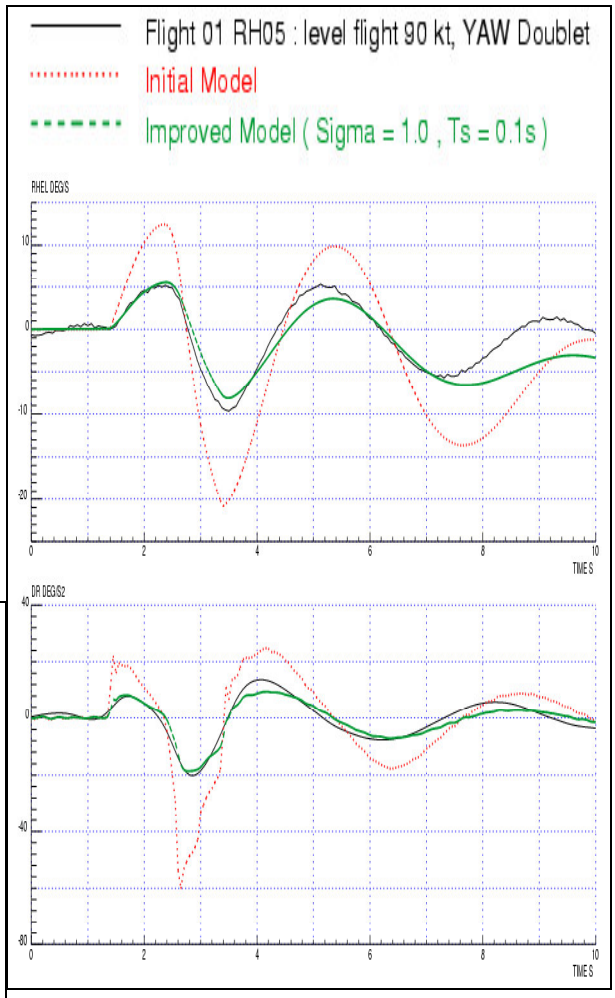

Figure 19 : Comparisons between HOST initial model and improved model at 90 kt.

The fact that the model provides good simulation, with meaningful physical values of (τ_s) and (σ), is a good indication of its physical consistency. Furthermore, the robustness or validity of the model is confirmed by comparisons with other flight test data : see Fig. 20 for a case at 140 kt (the simulation is slightly better with σ = 1.2 than with σ = 1).

The transition law (k(ε)) could probably be refined in order to better take into account the deviated airspeed through the fenestron in forward flight, (Fig. 1 shows for example that even at 150 kt, a significant part of the upstream airflow is deviated into the fenestron).

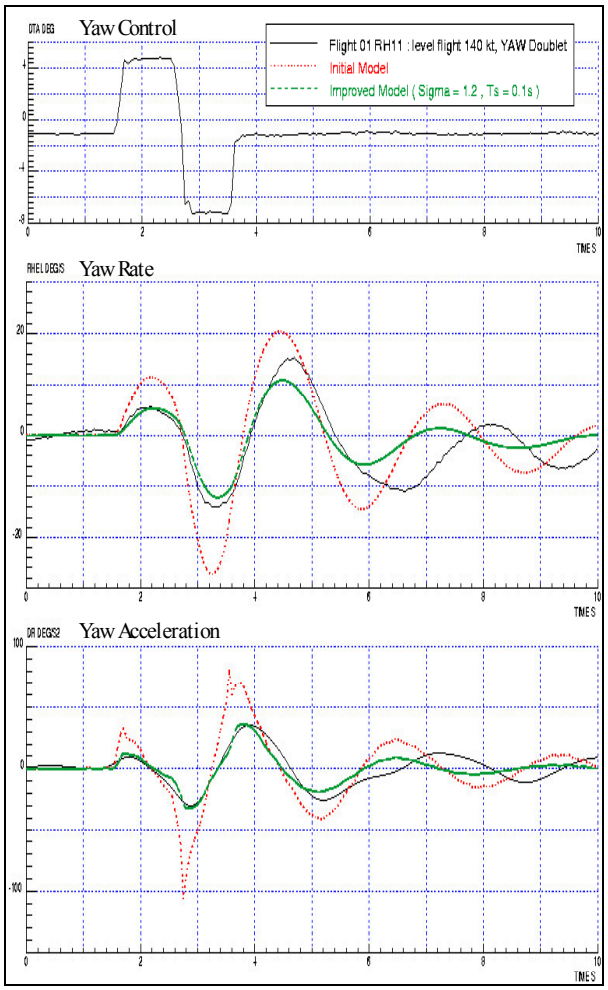

Figure 20 : Comparisons between HOST initial model and improved model at 140 kt.

Conclusions

The issue of the modelling of the fenestron for helicopter flight dynamics has been investigated. A new analytical model has been proposed in this paper. It improves significantly the simulation of the yaw dynamic response to pedal inputs which was overestimated by the previous models. The new proposed concept of the airflow behaviour through the fenestron leads to a model which is valid from hover up to high forward speeds. Moreover this better agreement with the Dauphin flight test data was obtained without any parametric tuning. The model parameters (like the rotor wake contraction factor), are let to their physical values as far as they are known.

This model of the fenestron thrust dynamics improves the prediction of the direct on-axis response to yaw control inputs. The longer term yaw axis dynamics could also be influenced by the inter-axis coupling (e.g. pitch – roll cross coupling) and by the interferences coming mainly from the main rotor wake. These next steps will be addressed within the GARTEUR HC-AG11 for investigating the prediction of the Dutch - Roll mode.

References

[1] R. Mouille : "«The Fenestron» shrouded tail rotor of the SA 341 Gazelle", Journal of the American Helicopter Society, October 1970

[2] R. Mouille, F. d'Ambra: "The fenestron a shrouded tail rotor concept for helicopters", 38th AHS forum, May 1986

|3] A. Vuillet, F. Morelli: "New aerodynamic design of the fenestron for improved performance", 12th European Rotorcraft Forum, Garmisch-Partenkirchen, RFA, September 1986

[4] A. Vuillet: "Operational advantages and power efficiency of the fenestron as compared to a conventional tail rotor", VERTIFLITE, July / August 1989

[5] R. W. Prouty: "The pros and cons of the fan-in-fin" Rotor and Wing 1992

[6] T. Renaud, C. Benoit, J.-C. Boniface, P. Gardarein : « Navier-Stokes computations of a complete helicopter configuration accounting for main and tail rotors effects », ERF Symposium, Friedrichshafen (Germany), September 16-18, 2003

[7] R. Ganesh Rajagopalan, C. N. Keys : « Detailed aerodynamic design of the RAH-66 FANTAIL using CFD », American Helicopter Society 49th annual forum, St Louis, Missouri, May 19-21 1993

[8] E. Alpman, L. N. Long, B. D. Kothmann : "Toward a better understanding of ducted rotor antitorque and directional control in forward flight " American Helicopter Society 59th annual forum, Phoenix, Arizona, May 6-8, 2003

[9] .B. N. Bourtsev, S. V. Selemenev : « Fan-in-fin performance at hover computational method », 26th European Rotorcraft Forum, The Hague, Netherlands, September 26-29 2000

[10] P. Krämer : « Parametric modeling approach to increase nonlinear fan-in-fin dynamic response simulation fidelity », 27th European rotorcraft forum, Moscow, Russia, 11-14 September 2001

[11] B. D. Kothmann, S. J. Ingle : « RAH-66 Comanche Linear Aeroservoelastic Stability Analysis : Model Improvements and flight test correlation » , Helicopter Society 54th annual forum, Washington, DC, May 20-22 1998

[12] M. Lazareff : « Aerodynamics of shrouded propellers », Paper D in “The Aerodynamics of VSTOL Aircraft”, AGARDograph 126, May 1968

[13] W. Johnson : « Helicopter Theory », Princeton University Press, Princeton, NJ, 1980

[14] D.A. Peters, N. HaQuang, "Dynamic inflow for practical applications", Journal of the American Helicopter Society, T. N., vol. 33, n° 4, pp. 64-68, October 1988

[15] D. Papillier, P. Large (CEV, France) ; P. Bonnet, B. Gimonet, D. Heuzé (ONERA,France) ; "The Dolphin 6075 : an Helicopter Dedicated to Flight Test Research” European Rotorcraft Forum", September 16-18, 1997